

Synthesis and Characterization of a Poly(1,3-dithienylisothianaphthene) Derivative for Bulk Heterojunction Photovoltaic Cells

D. L. Vangeneugden and D. J. M. Vanderzande

Laboratory of Organic and Polymer Chemistry, Institute for Material Research,
Division Chemistry, University Campus, Limburg University, B-3590 Diepenbeek, Belgium

J. Salbeck[†]

FB 6 Chemistry-Geography, Electrochemistry and Optoelectronic Materials,
Gerhard-Mercator-University Duisburg, Lotharstr. 1, D-47048 Duisburg, Germany

P. A. van Hal and R. A. J. Janssen*

Laboratory of Macromolecular and Organic Chemistry, Eindhoven University of Technology,
P.O. Box. 513, 5600 MB Eindhoven, The Netherlands

J. C. Hummelen

Stratingh Institute and MSC, University of Groningen, Nijenborgh 4, 9747 AG Groningen, The Netherlands

C. J. Brabec, S. E. Shaheen, and N. S. Sariciftci

Linz Institute for Organic Solar Cells (LIOS), Physical Chemistry, Johannes Kepler University Linz,
Altenbergerstr. 69, A-4040 Linz, Austria

Received: August 9, 2001

The synthesis of a poly(1,3-dithienylisothianaphthene) (PDTITN) derivative obtained via oxidative polymerization of 5,6-dichloro-1,2-bis(3'-dodecylthienyl)isothianaphthene is described. PDTITN exhibits a band gap of 1.80–1.85 eV. The redox properties of PDTITN were characterized using cyclic voltammetry and spectroelectrochemistry. Photoexcitation of PDTITN results in photoluminescence (PL) in the near-IR region and the formation of a triplet state. In the presence of a methanofullerene (PCBM) as an electron acceptor, PL and triplet formation of PDTITN are quenched. In photovoltaic devices using blends of the polymer with PCBM, the observed incident-photon-to-collected-electron efficiency (IPCE) up to 24% at 400 nm and the 3 orders of magnitude increase of short circuit current as compared to the polymer alone prove the photoactivity of the PDTITN/PCBM blend in the device.

Introduction

Composite films of semiconducting polymers as donors and molecular electron acceptors such as fullerenes have been used to construct "bulk-heterojunction" polymer photovoltaic cells.^{1–5} The primary step in these devices is a fast photoinduced charge-transfer reaction at the donor–acceptor interface, which results in a metastable charge-separated state.^{6–8} The nanoscopic interpenetrating network of the two constituents in a bulk heterojunction photovoltaic cell ensures a large interfacial area and, thus, an efficient charge generation. Photovoltaic power conversion efficiencies (η_e) of 2.5% under AM1.5 illumination have recently been reported for a bulk heterojunction solar cell consisting of a poly(2,5-dialkoxy-1,4-phenylene vinylene) as a donor and a methanofullerene as acceptor.⁹ Further improvement of these devices may be achieved by optimizing the absorption of light and the selective transport of charges.

At present, the mostly used materials such as substituted poly(*p*-phenylene vinylene)s and polythiophenes in polymer pho-

tovoltaic cells exhibit optical band gaps of $E_g = 1.9–2.2$ eV. Hence, the use of low band gap ($E_g < 1.8$ eV) polymers^{10,11} shall allow for an improved overlap of the polymer absorption spectrum with the solar emission and an enhancement in photon harvesting.

Here we describe a novel conjugated polymer (PDTITN, Scheme 1) with a poly(1,3-dithienylisothianaphthene) backbone. This polymer can be regarded as a regular copolymer of poly(3-alkylthiophene) (P3AT) and poly(isothianaphthene) (PITN). Although P3ATs have a band gap at 1.9–2.0 eV, PITN possesses a considerably lower band gap at 1.1 eV.^{12–16} By combining the structural characteristics of P3AT and PITN in the novel copolymer PDTITN, we have designed a material that possesses an intermediate optical band gap ($E_g = \sim 1.8$ eV).

We have investigated the electrochemical and photophysical properties of PDTITN as is and in combination with a methanofullerene derivative (PCBM,¹⁷ Chart 1) as an electron acceptor using photoinduced absorption spectroscopy (PIA). Both, the high IPCE value (24%) and the 3 orders of magnitude increase of short circuit current in the composite films prove the

* To whom correspondence should be addressed.

[†] FB 18 Physics, Macromolecular Chemistry and Molecular Materials, University Kassel, Heinrich-Plett-Str. 40, D-34109 Kassel, Germany

SCHEME 1

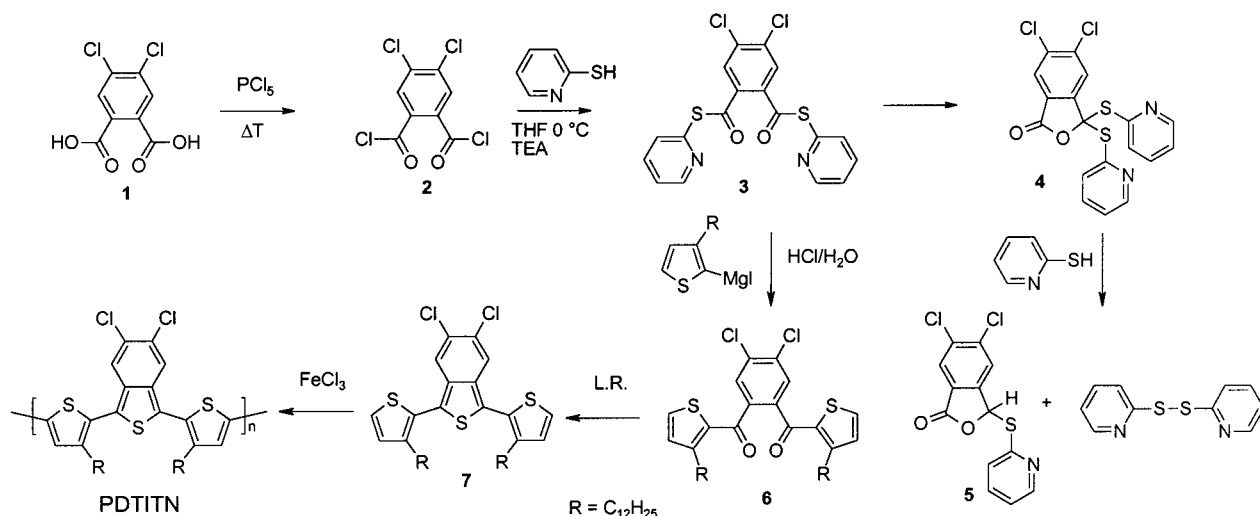
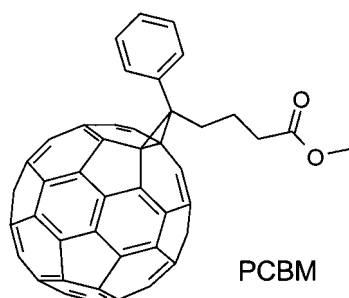


CHART 1



enhanced photoactivity of the PDTITN/PCBM blend inside the device.

Results

Synthesis of PDTITN. The synthesis of the poly(1,3-dithienylisothianaphthene) (PDTITN) derivative is outlined in Scheme 1. The synthesis of the monomer starts from 4,5-dichlorophthalic acid **1**, which is heated with two equivalents of PCl_5 to afford 4,5-dichlorophthalic acid chloride **2**. Compound **2** was subsequently allowed to react with mercaptopyridine to obtain 4,5-dichloro-1,2-di(S-(2-pyridyl))-benzenedithioate **3**. This dithioester is not stable in solution and slowly isomerizes into 3,3-di(S-pyridyl)-3H-5,6-dichloro-isobenzofuran-1-one **4**. This isomerization process has been previously encountered for related compounds.¹⁸ The isomerization is considerably accelerated upon heating and when an excess of mercaptopyridine is present, **4** is further transformed into 3-(S-pyridyl)-3H-5,6-dichloroisobenzofuran-1-one **5** and pyridyl disulfide through a radical scavenging process. The isomerization can be limited by adding **2** to a cold solution of mercaptopyridine and triethylamine (TEA) in THF and quenching the reaction immediately with diluted aqueous HCl (1 M). Because the lactones **4** and **5** are soluble in diethyl ether but the dithioester **3** is not, the desired product can be separated from the side products by recrystallization from dichloromethane/diethyl ether. The yield of this reaction is about 80%. 4,5-Dichloro-1,2-bis(3'-dodecylthienyl)-benzene **6** was obtained using the Grignard reagent of 2-iodo-3-dodecylthiophene in a yield of 66%. The 3-dodecylthiophene used in this reaction was synthesized via Grignard coupling reaction of 3-bromothiophene with dodecylmagnesium bromide by $\text{NiCl}_2(\text{dppp})$, analogously to literature procedures.¹⁹ Subsequent iodination with iodine and mercuric oxide in benzene

afforded the 2-iodo-3-dodecylthiophene in a yield of 74%.²⁰ Ring closure of diketone **6** with Lawesson's reagent resulted in 5,6-dichloro-1,3-bis(3'-dodecylthienyl)-isothianaphthene **7**. The polymerization of **7** was achieved by using anhydrous FeCl_3 at room temperature under nitrogen atmosphere.^{21,22} Work up involved Soxhlet extraction, using methanol and acetone to remove oligomers and dissolving the residue in chloroform. The chloroform solution was evaporated to dryness in vacuo, and the material was considered as the soluble polymer fraction (60%) which was used for further studies. The combined methanol and acetone extracts were evaporated, redissolved in chloroform, and washed with diluted HCl (1 N) to remove the iron salts. The organic layer was dried with MgSO_4 and evaporated to yield the oligomeric fraction (34%).

Characterization of PDTITN. GPC measurements, performed in THF relative to narrow low molecular weight polystyrene standards, indicated a limited molecular weight of $M_w = 6511$ g/mole and a polydispersity index of $\text{PDI} = 3.47$. For poly(3-alkylthiophenes), obtained by oxidative polymerization of 3-alkylthiophenes with FeCl_3 , molecular weights ranging from 30 000 to 300 000 g/mole with PDI from 1.3 to 5 have been reported.²³ However, when bithiophene or terthiophene derivatives are oxidatively polymerized, chemically or electrochemically, considerable lower molecular weights are obtained.^{21,23–25} The reduced M_w is explained by the reduced reactivity extended monomers compared with thiophenes, and this because of the stabilization of the corresponding radical cations involved in the polymerization.¹⁰ Side chain effects can play an important role in this context. Electron withdrawing groups will generally increase the reactivity, whereas electron-donating groups will stabilize the radical cations. For the latter, this causes a lowering of the monomer and oligomer reactivities and hence results in a decrease of the molecular weight of the corresponding polymers.^{26–29}

The thermal stability of the polymer was investigated by thermogravimetric analysis (TGA). Measurements were performed under a constant argon flow with a heating rate of 10 °C/min ranging from room temperature to 900 °C. The decomposition temperatures, as determined from the maximum of the differential thermogram (T_{DTG}) and as the temperature at which 5% of the original weight was lost ($T_{5\%}$), are 442 and 338 °C, respectively.

One of the difficulties of the FeCl_3 polymerization is the removal of the iron salts after polymerization.³⁰ Often large excesses of oxidant are needed, resulting in substantial amounts

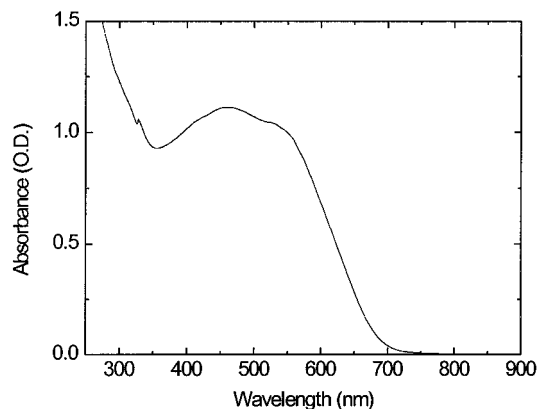


Figure 1. Absorption spectrum of PDTITN on quartz.

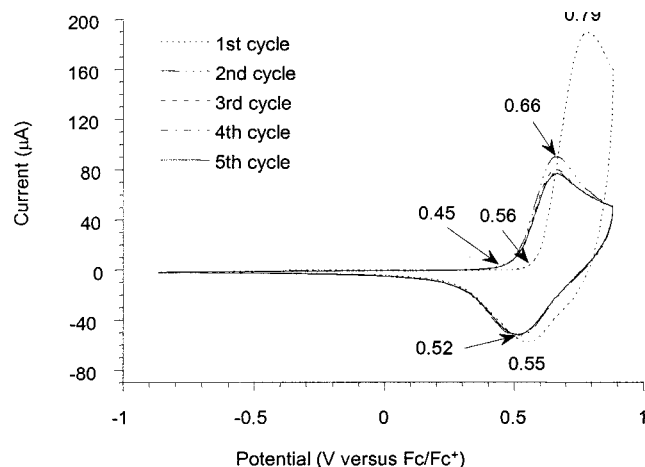


Figure 2. Cyclic voltammogram (five consecutive cycles, 10 mV/s) of PDTITN on Pt in acetonitrile (0.1 M TBAH). Potential versus Fc/Fc^+ .

of iron salts to be removed to obtain pure polymeric material. Soxhlet extraction with MeOH removes most of the doping by iron salts but small amounts may remain present in the material.²³ Atomic absorption spectroscopy (AAS) measurements indicated that the residual iron content is highest for the insoluble polymer fraction (0.1–3%), whereas lower amounts are detected for the oligomeric and soluble polymer fractions. For the present polymer, the residual iron content is 0.10%.

The absorption spectra of thin films of PDTITN differ slightly from film to film. The onset of the absorption is at about 670–690 nm (1.80–1.85 eV), with a broad maximum at about 458–468 nm (2.65–2.71 eV; Figure 1).

Cyclic Voltammetry and Spectroelectrochemistry. For cyclic voltammetry (CV), a thin film of PDTITN was deposited on the Pt working electrode by dip coating. Figure 2 displays the cyclic voltammograms of five consecutive scans, whereas no further changes in the CV occurred after the second scan. The optical band gap (1.80–1.85 eV) as observed from the onset in Figure 1 does not match the difference of oxidation and reduction potentials determined from electrochemistry, even for the onset values (0.45 + 1.93 = 2.38 eV).

By means of spectroelectrochemical (SPEL) measurements,^{31–36} the spectral changes upon electrochemical doping of the PDTITN films were investigated. Spectra recorded at intermediate doping levels are gathered in Figure 3. At high doping levels, two broad near-IR bands at 923 (1.34) and 1460 nm (0.85 eV) are dominating. These in the gap absorptions are generally indicative for polaron/bipolaron type relaxations of the polymer electronic structure upon doping.

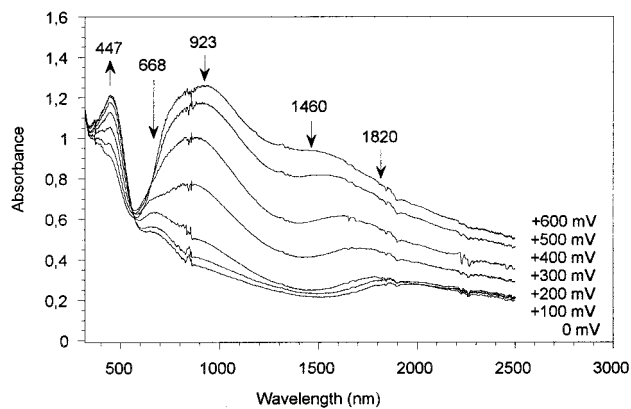


Figure 3. Spectroelectrochemical measurements of PDTITN on ITO in acetonitrile (0.1 M TBAH). Gradual reduction from +600 to 0 mV vs Fc/Fc^+ .

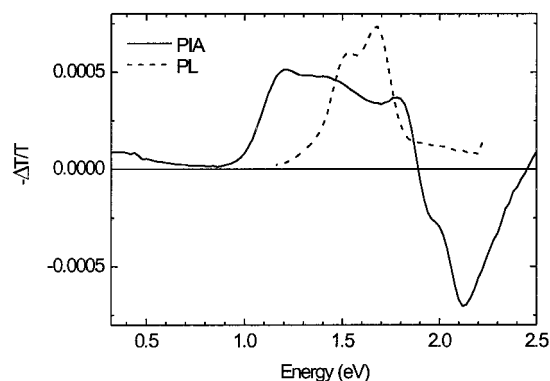


Figure 4. PIA and PL spectra of PDTITN on quartz. Data were recorded at 80 K by excitation at 2.54 eV (488 nm, 25 mW) and a modulation frequency of $\omega = 275$ Hz.

TABLE 1: Results of Fitting Intensity Dependence ($-\Delta T \propto I^\alpha$) and Frequency Dependence ($-\Delta T \propto \omega^{-x}$, Figure 5) for PIA Bands of PDTITN

position (eV)	α	x	position (eV)	α	x
0.4	0.6	-0.4	1.8	0.7	-0.2
1.2	0.8	-0.1	2.1	0.8	-0.3
1.4	0.8	-0.1			

The absorption spectra recorded for a thin film of PDTITN on quartz after chemical doping using nitrosonium tetrafluoroborate agree well with those observed by spectroelectrochemistry under high oxidation conditions.

Photoexcited Spectroscopy. The CW-modulated photoinduced absorption (PIA) spectrum of a thin film of PDTITN (Figure 4) at 80 K reveals a number of optical signatures. A small peak is found at 0.3 eV, and a much stronger broad peak is present starting at 1.2 eV and extending to 1.8 eV. Bleaching transitions are found at 2.0 (shoulder) and 2.1 eV (peak). In addition to the PIA, there is a weak, but clear, signature of photoluminescence (PL). The PL peaks are at 1.67 and 1.53 eV. The excitation pump intensity dependence of the PIA peaks follows a power law ($-\Delta T \propto I^\alpha$) with exponents α considerably higher than 0.5 (Table 1), indicating monomolecular decay processes ($-\Delta T \propto I$) dominate the relaxation. The modulation frequency dependences displayed in Figure 5 are numerically summarized in Table 1 by fitting a power-law ($-\Delta T \propto \omega^{-x}$) to the experimental curves.

Photoexcited spectroscopy on a composite film of PDTITN and PCBM (1:1 by weight) measured under the same conditions reveals that the spectrum of the blend is completely different from that of the individual compounds (Figure 6), whereas the

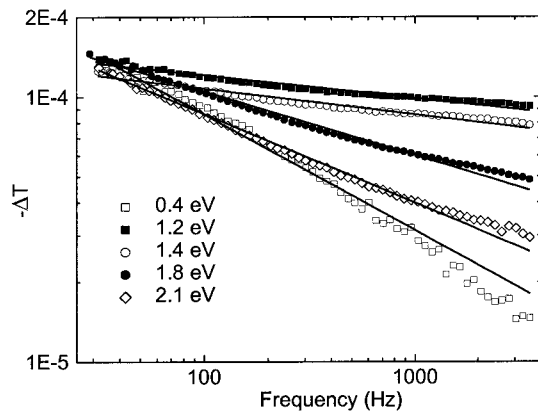


Figure 5. Semilogarithmic plot of the PIA signals of PDTITN as a function of the modulation frequency ω . Data were recorded at 80 K by excitation at 2.54 eV (488 nm, 25 mW). Solid lines represent fits to a power law ($-\Delta T \propto \omega^{-x}$, Table 1).

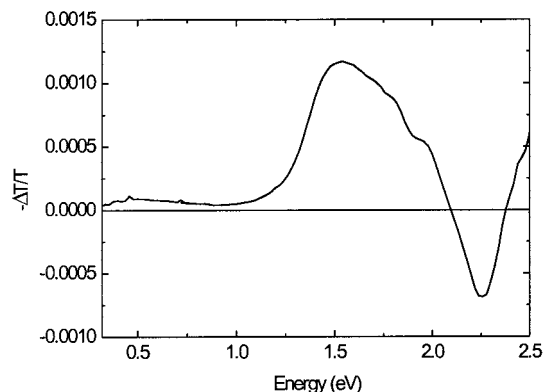


Figure 6. PIA spectrum of PDTITN/PCBM (1:1 w/w) composite film on quartz. Data were recorded at 80 K by excitation at 2.54 eV (488 nm, 25 mW) and a modulation frequency of $\omega = 275$ Hz.

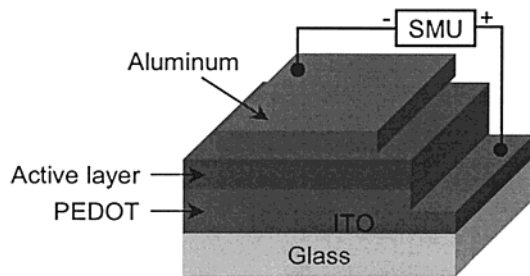


Figure 7. Schematic layout of the photodiodes used.

TABLE 2: Results of Intensity Dependence ($-\Delta T \propto I^\alpha$) PIA for Bands of PDTITN/PCBM

position (eV)	α	position (eV)	α
0.5	0.5	1.8	0.8
1.5	0.7	2.3	0.8

photoluminescence is almost completely quenched. The observed excitation intensity dependence of the PIA band can be fitted to power law, and the results are compiled in Table 2. The photoexcitation pump intensity dependence as well as the observed lifetime are different for 0.5 eV band. The 0.5 eV peak corresponds to a long-lived photoexcitation with bimolecular relaxation, whereas the other bands in the PIA spectrum correspond to shorter-lived species.

Photovoltaic Cells. Photovoltaic cells consisted of an active layer sandwiched between an ITO front electrode covered with a PEDOT:PSS conducting polymer layer and an Al back electrode (Figure 7). For devices containing PDTITN, we used

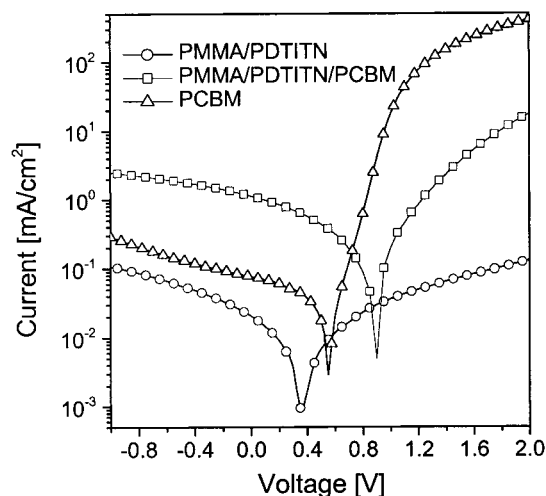


Figure 8. Semilogarithmic plot of the I/V characteristics of three devices under illumination with 80 mW/cm² from a solar simulator. Pristine devices from PDTITN (circles) were spun from a PMMA/PDTITN (2:3) solution to a thickness of ~ 90 nm, whereas PCBM (triangles) was spun directly from solution to a comparable thickness. The thickness of the device from PMMA/PDTITN/PCBM (1:2:6) (squares) was ~ 100 nm as determined by alpha stepper measurements. The measurement temperature was 50 °C.

TABLE 3: Photovoltaic Performance of Devices of PMMA/PDTITN (2:3), PCBM, and PMMA/PDTITN/PCBM (1:2:6)^a

	V_{oc} (mV)	I_{sc} ($\mu A/cm^2$)	FF (%)	AM1.5 η_e (%)
PDTITN	360	21	24	0.0023
PCBM	565	77	38	0.021
PDTITN/PCBM	880	1128	25	0.31

^a Data were recorded under illumination with a solar simulator with 80 mW/cm².

poly(methyl methacrylate) (PMMA) as a host matrix to improve the film forming properties. Figure 8 shows the I/V curve of a solar cell with an active layer consisting of a spin cast composite film of PMMA/PDTITN/PCBM (1:2:6 w/w/w) compared to the performance of devices from pristine PCBM and from PMMA/PDTITN (2:3 w/w). The photovoltaic characteristics of the devices (energy conversion efficiency η_e , fill factor FF, and incident photon to current efficiency IPCE) are given in Table 3. The device parameters were calculated using the following equations:

$$\eta_e[\%] = \frac{V_{oc}[V]I_{sc}[A/cm^2]FF}{P_{in}[W/cm^2]} \quad (1)$$

$$FF = \frac{V_p I_p}{V_{oc} I_{sc}} \quad (2)$$

$$IPCE[\%] = \frac{1240 I_{sc}[\mu A/cm^2]}{\lambda[nm]I[W/m^2]} \quad (3)$$

in which V_{oc} is the open circuit voltage, I_{sc} is the short-circuit current, λ is the excitation wavelength, I is the monochromatic light intensity, P_{in} is the intensity of AM1.5 light from a solar simulator, and V_p and I_p are the voltage and current at the maximum power point of the I/V curve.

Devices containing PDTITN showed a relative low fill factor (FF = 0.25) and rather low or even negligible rectification. This was also found for the PMMA/PDTITN device. Conversely,

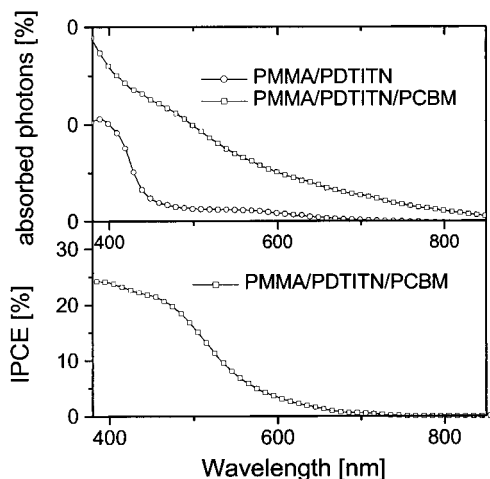


Figure 9. (a) Percentage of absorbed photons in thin films spun from solutions of PMMA/PDTITN (2:3) and PMMA/PDTITN/PCBM (1:2:6), respectively. Films were spun from the same solutions as the corresponding devices characterized in Figure 8 on cleaned glass slides, and absorption measurements were performed in transmission geometry. (b) Incident photons to converted electrons efficiency (IPCE) of a PMMA/PDTITN/PCBM (1:2:6) device, recorded at room temperature.

the PCBM diode shows a higher fill factor ($FF = 0.38$) and more than 3 orders of rectification at ± 2 V. Additionally, the electron injection at forward bias ($+2$ V) is more than 1 order of magnitude higher compared to that of the PMMA/PDTITN/PCBM device and more than 3 orders of magnitude higher compared to that of the PMMA/PDTITN device.

Mixing PCBM with PDTITN increases the short circuit current of the device compared to the value for the PMMA/PDTITN device by 1 order of magnitude. The overall power conversion efficiency of the PMMA/PDTITN/PCBM device was measured to be 0.3% under AM1.5 simulated light with 80 mW/cm^2 , whereas the pristine PCBM and the PMMA/PDTITN devices show 0.021 and 0.0023% efficiency, respectively.

Figure 9a shows the absorption spectrum of spin cast films from the polymer and the polymer/methanofullerene embedded in PMMA. Films were cast on glass from the same solutions as those used for device production. In Figure 9b, the incident photon to converted electron efficiency for the PMMA/PDTITN/PCBM device is plotted.³⁷

The highest IPCE value, almost 24%, was observed in the high-energy region around 400 nm. The monochromatic quantum efficiency of the device at 400 nm is calculated with 5.3%, assuming a V_{oc} of 880 mV, a FF of 0.25, and an IPCE of 24%.

Discussion

Although it is clear from the PIA experiments described above that there are major differences between the photoexcitations generated in pure PDTITN and those generated in the PDTITN/PCBM blend, the actual interpretation is less straightforward. The PIA spectrum of the pure PDTITN has strong similarities to the PIA spectrum of poly(3-hexylthiophene).³⁸ The most likely explanation is that the strong transition in the region from 1.1 to 1.9 eV corresponds to a triplet-triplet absorption. The lifetime of this photoexcited triplet state is less than 100 μs . The intensity exponents ($\alpha = 0.8$) for the most prominent peaks (1.2 and 1.4 eV) are fully consistent with this assignment. A considerable quenching of the PDTITN fluorescence occurs in the PDTITN/PCBM blend, and the PIA spectrum has a blue shifted maximum at 1.5 eV instead of 1.2 eV compared to that of the pure PDTITN. In principle, one could envisage two

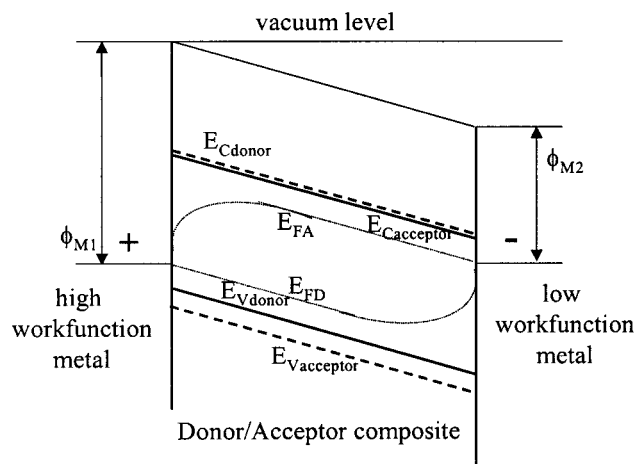


Figure 10. Schematic drawing of the potentials inside a donor/acceptor bulk heterojunction solar cell. E_{FD} and E_{FA} are the quasi-Fermi levels of the donor and the acceptor, respectively; E_C and E_V are the conduction and the valence band of the single materials.

possibilities to explain these differences: either electron transfer from the polymer to the methanofullerene or, alternatively, energy transfer. What is the nature of the peak at 1.5 eV in the PDTITN/PCBM film? One possibility is to assign this band to a triplet-triplet absorption of the PCBM. In solution, the triplet spectrum of PCBM gives a triplet-triplet absorption at 1.7 eV with a shoulder at 1.5 eV.³⁹ The lowest neutral excited state in a PDTITN/PCBM blend is probably the triplet state of PCBM, estimated to be at about $E^* = 1.50\text{--}1.60$ eV above the ground state, based on comparison with C_{60} and *N*-methyl-fulleropyrrolidine.^{40–42} The reduction potential (A_A) of PCBM in dichloromethane is -1.0 V against Fc/Fc^+ . With the lowest-energy excited state at $E^* = 1.50\text{--}1.60$ eV, the oxidation potential should be less than approximately $1.55 - 1.0 = +0.55$ eV against Fc/Fc^+ . From the oxidation potential measured for PDTITN, the onset value that is found is $+0.56$ V in the first cycle and $+0.45$ V in subsequent cycles, i.e., just on the borderline. This simple calculation, not taking into account the Coulombic effects, suggests that the charge-transferred state will not be stabilized energetically and may efficiently relax by a fast back transfer.

In the solar cell devices, the situation is different. Upon applying a top and a bottom metal contact with different work functions, as it is the case for the photovoltaic devices, an internal electrical field may be generated. An upper limit for this field inside the two-component system is given by the built-in potential of the system divided by the thickness of the active layer. For photovoltaic devices, the built-in potential may be estimated from the open circuit voltage (i.e., the difference of the quasi-Fermi levels). Although this approximation is only valid for low temperatures, the error is usually small (i.e., $<10\%$). By assuming further that the field distribution is homogeneous and by neglecting interface effects (non rectifying metal contacts in the sense of a space charge region), the internal electrical field (E_{bi}) in the device consisting of an PDTITN/PCBM active layer, embedded between ITO/PEDOT and Al electrodes, may be estimated by the following equation:

$$E_{bi} = V_{oc}/d \quad (4)$$

where d is the thickness of the active layer. A schematic drawing of the relevant potentials is given in Figure 10. From Figure 10, it is also clear that the region over which the electrical field is developed may be smaller than the device thickness. With

an V_{oc} of 880 mV and a thickness of 100 nm, the internal field for the PDTITN/PCBM devices is estimated by 8.8×10^5 V/cm. Fields of this strength are well-known to trigger photoinduced charge transfer reactions which would be otherwise thermodynamically limited.^{43,44}

The occurrence of photoinduced charge transfer between PDTITN and PCBM inside the photovoltaic devices is evidenced by the huge increase in short circuit current for this device compared to the devices with single-component active layers as denoted in Table 3. Further evidence for photoinduced charge transfer comes from evaluation of the spectrally resolved photocurrent. Both the high IPCE value (24%) as well as the shape of the IPCE curve versus wavelength prove the photoactivity of the two components inside the device.

Experimental Section

General Remarks and Instrumentation. Unless stated otherwise, commercial products were of analytical grade and used without further purification. Solvents were dried and distilled prior to use. THF and Et₂O were distilled over sodium/benzophenone, and CHCl₃, CH₂Cl₂, and DMSO were dried over molecular sieves (4 Å) before distillation. Reactions were carried out under inert (N₂) atmosphere. Column chromatography was carried out over silica gel (Merck Kieselgel 60) using eluents indicated. ¹H NMR spectra were recorded in CDCl₃ at 400 MHz on a VARIAN Inova spectrometer using a 5 mm probe. Chemical shifts (δ) in ppm are reported relative to tetramethylsilane (TMS) and were determined relative to the residual nondeuterated solvent absorption (CHCl₃). The chemical shift of CHCl₃ is, according to convention, situated at 7.24 ppm relative to tetramethylsilane (TMS). The ¹³C NMR experiments were recorded at 100 MHz on the same spectrometer using a 5 mm broadband probe. Chemical shifts were determined relative to the ¹³C resonance shift of CHCl₃ (77.0 ppm relative to TMS). Chemical shifts could be assigned on the basis of the shift values, coupling patterns, integration, attached proton test (ATP), and two-dimensional techniques as COSY (¹H–¹H), HETCOR (¹H–¹³C) optimized for ¹J_{CH} = 8 Hz (direct) and ³J_{CH} = 140 Hz (long range), and INADEQUATE (¹³C–¹³C) optimized for ¹J_{CC} = 48 Hz. Direct insert probe mass spectrometry (DIP-MS) analyses were carried out on a Finnigan TSQ 70. Analyses were carried out in the electron impact mode (EI, electron energy of 70 eV) and the chemical ionization mode (CI, 3000–4000 mTorr *i*-butane). GC-MS measurements (Gas Chromatography Mass Spectrometry) were performed using a Thermo Quest Voyager GC/MS apparatus. Fourier transform infra red spectroscopy (FT-IR) was performed on a Perkin-Elmer 1600 FT-IR apparatus. Melting points were determined on an Electrothermal 9100. Gel permeation chromatography (GPC) measurements were performed on a Spectra Physics Spectra Series P100 equipped with a PLgel 5 μ column (Polymer Labs) and a refractive index RI-71 detector (Shodex). Molecular weights were determined in THF solution relative to narrow distribution low molecular weight polystyrene standards (Polymer Labs). Thermogravimetric analysis (TGA) was performed on a TA Instrument 951 thermogravimetric analyzer under a continuous argon-flow of 80 mL/min. Residual iron contents were determined by atomic absorption spectroscopy (AAS) on a Perkin-Elmer 1100 B flame atomic absorption spectrophotometer. UV–vis–near-IR spectra were recorded on a Perkin-Elmer Lambda 900 spectrophotometer.

Cyclic Voltammetry. The electrochemical setup consisted of a Metrohm cell equipped with a Pt disk working electrode, a glassy carbon counter electrode and a Ag/AgCl or SCE

reference electrode connected to an EG&G Princeton potentiostat/galvanostat model 273. The measurements were performed under nitrogen in dried and degassed acetonitrile and dichloromethane solutions. Tetrabutylammonium hexafluorophosphate (TBAH) was used as inert electrolyte in a concentration of 0.1 M. After each measurement, an internal calibration versus the Fc/Fc⁺ couple was performed, and all potentials are given relative to Fc/Fc⁺. Cyclic voltammograms of the polymer were taken from films deposited on the surface of the working electrode by means of dip coating from a dichloromethane solution. These measurements were performed in an acetonitrile electrolyte solution, generally at a scan rate of 10 mV/s.

Spectroelectrochemistry. A thin-layer spectroelectrochemical cell was used.⁴⁵ The thin-layer cell contained a transparent ITO working electrode, an Ag/AgCl pseudo-reference electrode, and a gold-coated stainless steel counter electrode. As for the cyclic voltammetry, all potentials are given relative to Fc/Fc⁺. The electrodes were connected to an EG&G Princeton scanning potentiostat model 362, and spectra were recorded with a Perkin-Elmer Lambda 9 UV–Vis–near-IR spectrophotometer. Measurements were performed on thin polymer films prepared by drop coating on the ITO working electrode. 0.1 M TBAH acetonitrile was used as electrolyte solution.

Chemical Doping of Films. Films of PDTITN were drop-cast from *o*-dichlorobenzene on quartz and subsequently dip-doped (oxidized) in acetonitrile containing nitrosonium tetrafluoroborate.

Photoinduced Absorption Spectroscopy. PIA spectra were recorded between 0.25 and 3.5 eV by exciting with a mechanically modulated cw Spectra Physics Ar-ion laser (488 nm, 275 Hz) pump beam and monitoring the resulting change in transmission of a tungsten–halogen probe light through the sample (ΔT) with a phase sensitive lock-in amplifier after dispersion by a triple grating Oriel 257 monochromator and detection, using Si, InGaAs, and cooled InSb detectors. The pump power incident on the sample was 25 mW with a beam diameter of 2 mm. The photoinduced absorption, $-\Delta T/T \approx \Delta\alpha d$, was directly calculated from the change in transmission after correction for the photoluminescence, which was recorded in a separate experiment. Photoinduced absorption spectra and photoluminescence spectra were recorded with the pump beam in an almost parallel direction to the probe beam. Samples were held at 80 K in an inert nitrogen atmosphere using an Oxford Optistat continuous flow cryostat; during measurements, the temperature was kept constant within ± 0.1 K. Films for PIA were prepared as follows. PDTITN was prepared by drop casting from *o*-dichlorobenzene solution onto a quartz substrate, which was preheated to 100 °C to enhance evaporation of the solvent. The resulting film had an optical density varying from 0.8 to 1.2 over the film. A film of PCBM was prepared by drop casting from *o*-dichlorobenzene on quartz. The film had an optical density of OD = 0.8 at 488 nm. A small peak at 711 nm (1.74 eV), characteristic for PCBM, marks the onset of the absorption spectrum. A composite film of PDTITN and PCBM 1:1 by weight was prepared from an *o*-dichlorobenzene solution by drop casting. The optical density varied between 2.0 and 2.7 over the film. The onset of the absorption is at about 705 nm (~ 1.76 eV, a PCBM absorption peak), with a maximum at about 460 nm (2.70 eV, a PDTITN absorption peak).

Production and Measurement of Photovoltaic Devices. ITO/glass substrates were cleaned in ultrasonic baths of acetone, methanol, and 2-propanol, followed by oxygen plasma treatment. Poly(ethylenedioxythiophene) doped with poly(styrenesulfonic acid) (PEDOT:PSS, Bayer AG) was spin-coated to a thickness

of 100 nm on top of the ITO from an aqueous solution. For the solar cells reported here, poly(methyl methacrylate) (PMMA) was used as host matrix because the molar mass of the PDTITN was too low to form homogeneous pinhole free thin films by solution casting. The weight ratio of the photoactive layer deposited by spin casting was PMMA:PDTITN:PCBM = 1:2:6. This weight ratio of 1:3 between the donor and the acceptor was recently found to be favorable for bulk heterojunction solar cells based on conjugated polymer/fullerene composites.^{46,47} Reference devices with pristine polymer and PCBM active layers were also prepared. Devices from PDTITN alone, processed by spin casting, did not form homogeneous and continuous films and were consequently short-circuited. Blending PMMA into PDTITN improved the film quality resulting in a photovoltaic response. However, it cannot be excluded that the performance of the PMMA/PDTITN device is still limited by poor film quality. Devices were spin cast from *o*-dichlorobenzene with an average film thickness of ~90–100 nm as determined by alpha-stepper measurements. Device fabrication was performed in a drybox under an argon atmosphere. The Al top electrode was evaporated thermally with a thickness of ~80 nm. A schematic layout of the devices is given in Figure 7.

I/V curves were recorded by a Keithley 2400 source meter in inert atmosphere at room temperature under illumination with 80 mW/cm² white light from a Steuernagel solar simulator. No corrections were made for the spectral mismatch between the solar simulator and the true AM1.5 spectrum. The measurement temperature was ~50 °C. Spectrally resolved photocurrent measurements were recorded by the lock-in technique, illuminating the device with ~0.2 mW/cm² monochromatized light with a fwhm of ~4 nm from a Xe arc lamp and white light background illumination in inert atmosphere. No noticeable degradation of the devices was observed during the measurement cycles. Light intensities were measured by a calibrated Si photodiode.

Synthesis

4,5-Dichlorophthalic Acid Chloride (2). Powdered 4,5-dichlorophthalic acid (20 g, 0.085 mol) and PCl₅ (35.5 g, 0.17 mol) are mixed in a reaction flask with a glass rod before heating to 160 °C. At a temperature of about 60 °C, the reaction starts quite vigorously and HCl is produced (CAUTION!). The evolving HCl vapor is directed through a basic solution to neutralize the acid. After 2 h of heating under reflux and vigorous stirring, the mixture is allowed to cool. Vacuum distillation gives **2** as a colorless liquid which crystallizes at room temperature. Yield 20.36 g (88%); mp 34 °C; bp 160 °C (0.9 mbar); IR (KBr, ν , cm⁻¹) 3097, 3077, 3021, 1785, 1768, 1735, 1581, 1535, 1460, 1216, 961, 791; MS (EI, *m/e*) 270 (M⁺), 235 (-Cl), 207 (-COCl), 172 (-Cl, -COCl), 144 (-2COCl), 109, 74; ¹H NMR 7.92 (s, 2H).

4,5-Dichloro-1,2-di(S-(2-pyridinyl))benzenedithioate (3). A solution of TEA (5 mL) and 2-mercaptopyridine (3.1 g, 27.9 mmol) and THF (50 mL) is stirred for 15 min at 0 °C. To this, a solution of **2** (3.8 g, 13.9 mmol) in THF (20 mL) is added, and the reaction is immediately worked up by the addition of HCl (1%, 200 mL). After extraction with CHCl₃, the combined fractions are washed with NaOH (10%), NaHCO₃ (1 M), and H₂O until neutral. Finally, **3** is obtained after drying over MgSO₄ and crystallization from CH₂Cl₂/diethyl ether. Yield 4.7 g (79%); mp 119 °C; IR (KBr, ν , cm⁻¹) 3077, 3050, 1694, 1673, 1573, 1561, 1539, 1449, 1419, 1212, 961, 808, 772; MS (EI, *m/e*) 420 (M⁺), 310 (-SPy), 282 (-COSPy), 172, 144, 109, 78; ¹H NMR 8.60 (dq, 2H), 7.93 (s, 2H), 7.72 (m, 4H), 7.29 (m, 2H).

3-Dodecylthiophene. Dodecylbromide (38.9 g, 0.156 mol) in diethyl ether (100 mL) is added dropwise to Mg (3.8 g, 0.156 mol) in Et₂O (50 mL), activated with a trace of iodine. After addition, the reaction mixture is refluxed for about 2 h. The obtained Grignard reagent is allowed to cool and subsequently added to a cooled mixture (0 °C) of 3-bromothiophene (17.0 g, 0.104 mol) and NiCl₂(dppp) (70 mg, 1.2 mmol) in Et₂O (100 mL). After stirring overnight at room temperature, the reaction is worked up by the slow addition of water (100 mL). The crude product is extracted with Et₂O and dried over MgSO₄. Purification is performed by means of column chromatography (silica gel, *n*-hexane). Yield 20.2 g (77%); IR (NaCl, ν , cm⁻¹) 2923, 2852, 1536, 1465, 1409, 1377, 1152, 1078, 858, 835, 769; MS (EI, *m/e*) 252 (M⁺), 111, 98 (-C₁₁H₂₂), 97 (-C₁₁H₂₃), 85, 55; ¹H NMR 7.23 (dd, 1H), 6.94 (d, 1H), 6.92 (d, 1H), 2.65 (t, 2H), 1.65 (p, 2H), 1.30 (m, 18H), 0.92 (t, 3H).

2-Iodo-3-dodecylthiophene. 3-Dodecylthiophene (14.9 g, 58.5 mmol) and I₂ (22.3 g, 87.8 mmol) are dissolved in benzene (60 mL) and cooled to 5 °C. Under continuous stirring, HgO (19.0 g, 87.8 mmol) is added in small portions over about 1 h until the dark brown-red color disappears and the mixture turns orange. The formed HgI is filtered off on a Buchner and washed with Et₂O (3 × 20 mL). The combined filtrates are washed with a Na₂S₂O₃ solution (0.65 N, 2 × 100 mL) and subsequently with brine (100 mL). After drying over MgSO₄, the crude reaction product is purified by means of column chromatography (silica gel, *n*-hexane). Yield 16.4 g (74%); IR (KBr, ν , cm⁻¹) 3103, 3070, 2952, 2914, 2848, 2729, 2676, 1529, 1465, 1397, 1375, 1225, 966, 828, 716, 684, 635; MS (EI, *m/e*) 378 (M⁺), 251 (-I), 223 (-C₁₁H₂₃), 137, 111, 97 (-I, -C₁₁H₂₂), 71, 57, 43; ¹H NMR 7.36 (d, 1H), 6.74 (d, 1H), 2.53 (t, 2H), 1.56 (p, 2H), 1.26 (m, 18H), 0.88 (t, 3H).

4,5-Dichloro-1,2-bis(3'-dodecylthienoyl)benzene (6). A solution of 2-iodo-3-dodecylthiophene (16.3 g, 43.1 mmol) in THF (20 mL) is slowly added to Mg (1.1 g, 45.3 mmol) in THF (30 mL), activated with a trace of iodine. After 2 h of reflux, the obtained Grignard reagent is added to a solution of dithioester **3** (7.9 g, 18.7 mmol) in THF (100 mL). The mixture is stirred for 30 min after which HCl (10%, 100 mL) is added. Further work up comprises extraction with Et₂O, washing of the combined extracts with NaOH (10%), NaHCO₃ (1 M) and H₂O and drying over MgSO₄. The crude product is finally purified by column chromatography (silica, CHCl₃/*n*-hexane 9/1) and **6** is obtained as a slightly yellow oil. Yield 8.7 g (66%); IR (KBr, ν , cm⁻¹) 3105, 3077, 3052, 2956, 2921, 2851, 1645, 1579, 1540, 1521, 1409, 1379, 1284, 1263, 1239, 1133, 970, 846, 721; MS (EI, *m/s*) 702 (M⁺), 451 (-DodTh), 309, 296, 283, 251 (DodTh⁺), 201, 137, 111, 97 (ThCH₂⁺), 71, 57, 41; ¹H NMR 7.73 (s, 2H), 7.45 (d, 2H), 6.98 (d, 2H), 2.80 (t, 4H), 1.52 (p, 4H), 1.23 (m, 36H), 0.86 (t, 6H).

5,6-Dichloro-1,2-bis(3'-dodecylthienyl)isothianaphthene (7). A mixture of 4,5-dichloro-1,2-bis(3'-dodecylthienoyl)-benzene **6** (8.45 g, 12.0 mmol) and Lawesson's reagent (LR) (5.45 g, 13.5 mmol) in CH₂Cl₂ (200 mL) is stirred at 50 °C. After an hour, the solvent is evaporated and ethanol (200 mL) is added. This mixture is refluxed again for 30 min. Subsequently, H₂O (300 mL) is added and the product extracted with CHCl₃ (3 × 100 mL). The combined fractions are washed with NaOH (10%) and water until neutral. After drying over MgSO₄, the solvent is evaporated and the crude product is purified by column chromatography (silica, CHCl₃). Finally, the product is dissolved in CHCl₃ and precipitated by adding an excess of *n*-hexane. After filtration the product is obtained as an orange powder. Yield 8.01 g (95%); IR (KBr, ν , cm⁻¹) 3105, 3064, 2923, 2852,

1592, 1461, 1436, 1367, 1309, 1099, 993, 871, 834, 720; MS (EI, m/s) 702 (M^+), 547 ($-C_{11}H_{23}$), 511, 357, 321, 297, 261, 137, 111, 97, 69, 57; 1H NMR 7.73 (s, 2H, H_4), 7.40 (d, 2H, H_5'), 7.07 (d, 2H, H_4'), 2.64 (t, 4H, H_{11}''), 1.60 (p, 4H, H_{12}''), 1.22 (m, 36H, $H_{33}''-H_{11}''$), 0.88 (t, 6H, H_{12}''); ^{13}C NMR 142.85 (C_3'), 135.02 (C_3a), 129.45 (C_4'), 129.41 (C_5), 126.59 (C_2'), 126.49 (C_3), 126.40 (C_5'), 121.69 (C_4), 31.92 (C_{10}''), 30.89 (C_2''), 29.67, 26.64, 29.56, 29.38 (C_5''), 29.36 (C_9''), 29.32 (C_3''), 29.00 (H_{11}''), 22.69 (C_{11}''), 14.13 (C_{12}''); UV-vis (λ_{max} (nm), ϵ) 283 (15 784), 405 (8395); fluorescence (λ_{max} (nm)) 531.

Polymerization.^{21,22} Polymerization is performed by adding five equivalents of powdery anhydrous $FeCl_3$ to a 0.07 M chloroform solution of the monomer. The reaction is carried out at room temperature and under nitrogen atmosphere, over 12 h. Work up consists of diluting the crude reaction mixture with chloroform after which methanol is added to precipitate the polymer. The product is collected in a Soxhlet extraction case by filtration and extracted with methanol and acetone, with each solvent until the extracts are completely colorless. The residue is dissolved in chloroform by stirring at room temperature over 30 min. Insoluble material is removed by filtration, dried, and considered as the insoluble polymer fraction (6%). The chloroform solution is evaporated to dryness in vacuo and the as such obtained material is considered as the soluble polymer fraction (60%). The combined methanol and acetone extracts are evaporated, redissolved in chloroform, and washed with diluted HCl (1 N) to remove the iron salts. The organic layer is dried with $MgSO_4$ and evaporated to yield the oligomeric fraction (34%).

Acknowledgment. The work performed in Diepenbeek was financially supported by the Flemish Government (IWT). The work in Eindhoven was supported by the Council for Chemical Sciences of The Netherlands Organization for Scientific Research (CW-NWO) and the Eindhoven University of Technology in the PIONIER program (98400). The work in Linz was performed within the Christian Doppler Society dedicated laboratory on Plastic Solar Cells funded by the Austrian Ministry of Economic Affairs and Quantum Solar Energy Linz Ges. m. b. H. The work was further supported by the "Fonds zur Förderung der wissenschaftlichen Forschung" of Austria (Project Nos. P-12680-CHE and M539-CHE), the Magistrat Linz, the Land Oberösterreich (ETP Wi(Ge)-200513/1), and The Netherlands Organization for Energy & Environment (NOVEM).

References and Notes

- Halls, J. J. M.; Walsh, C. A.; Greenham, N. C.; Marseglia, E. A.; Friend, R. H.; Moratti, S. C.; Holmes, A. B. *Nature* **1995**, *376*, 498.
- Yu, G.; Gao, J.; Hummelen, J. C.; Wudl, F.; Heeger, A. J. *Science* **1995**, *270*, 1789.
- Yu, G.; Heeger, A. J. *J. Appl. Phys.* **1995**, *78*, 4510.
- Roman, L. S.; Andersson, M. R.; Yohannes, T.; Inganäs, O. *Adv. Mater.* **1997**, *9*, 1164.
- Granström, M.; Petrisch, K.; Arias, A. C.; Lux, A.; Lux, M.; Andersson, M. R.; Friend, R. H. *Nature* **1998**, *395*, 257.
- Sariciftci, N. S.; Smilowitz, L.; Heeger, A. J.; Wudl, F. *Science* **1992**, *258*, 1474.
- Smilowitz, L.; Sariciftci, N. S.; Wu, R.; Gettinger, C.; Heeger, A. J.; Wudl, F. *Phys. Rev. B* **1993**, *47*, 13835.
- Meskers, S. C. J.; van Hal, P. A.; Spiering, A. J. H.; Hummelen, J. C.; van der Meer, A. F. G.; Janssen, R. A. J. *Phys. Rev. B* **2000**, *61*, 9917.
- Shaheen, S. E.; Brabec, J. C.; Padinger, F.; Fromherz, T.; Hummelen, J. C.; Sariciftci, N. S. *Appl. Phys. Lett.* **2001**, *78*, 841.
- Roncali, J. *Chem. Rev.* **1997**, *97*, 173.
- Pomerantz, M. In *Handbook of Conducting Polymers*, 2nd ed.; Skotheim, T. A., Elsenbaumer, R. L., Reynolds, J. R., Eds.; Marcel Dekker Inc.: New York, 1998; p 277.
- Wudl, F.; Kobayashi, M.; Heeger, A. J. *J. Org. Chem.* **1984**, *49*, 3382.
- Hoogmartens, I.; Adriaensens, P.; Vanderzande, D.; Gelan, J.; Quattrocchi, C.; Lazzaroni, R.; Brédas, J. L. *Macromolecules* **1992**, *25*, 7347.
- Hoogmartens, I.; Adriaensens, P.; Carleer, R.; Vanderzande, D.; Martens, H.; Gelan, J. *Synth. Met.* **1992**, *51*, 219.
- Kiebooms, R.; Hoogmartens, I.; Adriaensens, P.; Vanderzande, D.; Gelan, J. *Macromolecules* **1995**, *28*, 4961.
- Zerbi, G.; Magnoni, M. C.; Hoogmartens, I.; Kiebooms, R.; Carleer, R.; Vanderzande, D.; Gelan, J. *Adv. Mater.* **1995**, *7*, 1027.
- Hummelen, J. C.; Knight, B. W.; LePeq, F.; Wudl, F.; Yao, J.; Wilkins, C. L. *J. Org. Chem.* **1995**, *60*, 532.
- Kiebooms, R. H. L.; Adriaensens, P. J. A.; Vanderzande, D. J. M.; Gelan, J. M. J. *J. Org. Chem.* **1997**, *62*, 1473.
- Van Pham, C.; Mark, H. B.; Zimmer, H. *Synth. Commun.* **1986**, *16*, 689.
- Uhlenbroek, J. H.; Bijloo, J. D. *Recl. Trav. Chim. Pays-Bas* **1960**, *79*, 1181.
- Andreani, F.; Salatelli, E.; Lanzi, M. *Polymer* **1996**, *37*, 661.
- Hanna, R.; Leclerc, M. *Chem. Mater.* **1996**, *8*, 1512.
- McCullough, R. D. *Adv. Mater.* **1998**, *10*, 93.
- Kaeriyama, K. In *Handbook of Organic Conductive Molecules and Polymers*; Nalwa, H. S., Ed.; Wiley: New York, 1996; Vol. 2.
- Konestabo, O. R.; Aasmundtveit, K. E.; Samuelsen, E. J.; Bakken, E.; Carlsen, P. H. *J. Synth. Met.* **1997**, *84*, 589.
- Zotti, G.; Gallazzi, M. C.; Zerbi, G.; Meille, S. V. *Synth. Met.* **1995**, *73*, 217.
- Zotti, G.; Marin, R. A.; Gallazzi, M. C. *Chem. Mater.* **1997**, *9*, 2945.
- Barbarella, G.; Zambianchi, M.; Di Toro, R.; Colonna, M. J.; Iarossi, D.; Goldoni, F.; Bongini, A. *J. Org. Chem.* **1996**, *61*, 8285.
- Fréchet, M.; Belletête, M.; Bergeron, J.-Y.; Durocher, G.; Leclerc, M. *Macromol. Chem. Phys.* **1997**, *198*, 1709.
- Abdou, M.; Lu, X.; Xie, Z. W.; Orfino, F.; Deen, M.; Holdcroft, S. *Chem. Mater.* **1995**, *7*, 631.
- Dobhofer, K.; Rajeshwar, K. In *Handbook of Conducting Polymers*, 2nd ed.; Skotheim, T. A., Elsenbaumer, R. L., Reynolds, J. R., Eds.; Marcel Dekker: New York, 1998; p 531.
- Trznadel, M.; Zagorska, M.; Lapkowski, M.; Louarn, G.; Lefrant, S.; Pron, A. *J. Chem. Soc., Faraday Trans.* **1996**, *92*, 1387.
- Trznadel, M.; Pron, A.; Zagorska, M.; Pielichowski, C. R. *J. Macromolecules* **1998**, *31*, 5051.
- Daub, J.; Feuerer, M.; Mirlach, A.; Salbeck, J. *Synth. Met.* **1991**, *41-43*, 1551.
- Leuning, J.; Uebe, J.; Salbeck, J.; Gherghel, L.; Wang, C.; Müllen, K. *Synth. Met.* **1999**, *100*, 79.
- Buvat, P.; Hourquebie, P. *Macromolecules* **1997**, *30*, 2685.
- Roman, L. S.; Mammo, W.; Pettersson, L. A. A.; Andersson, M. R.; Inganäs, O. *Adv. Mater.* **1998**, *10*, 774.
- Van Hal, P. A.; Christiaans, M. P. T.; Wienk, M. M.; Kroon, J. M.; Janssen, R. A. J. *J. Phys. Chem. B* **1999**, *103*, 4352.
- Janssen, R. A. J.; Hummelen, J. C.; Wudl, F. *J. Am. Chem. Soc.* **1995**, *117*, 544.
- Williams, R. M.; Zwier, J. M.; Verhoeven, J. W. *J. Am. Chem. Soc.* **1995**, *117*, 4093.
- Thomas, K. G.; Biju, V.; George, M. V.; Guldi, D. M.; Kamat, P. V. *J. Phys. Chem. A* **1998**, *102*, 5341.
- Guldi, D. M.; Maggini, M.; Scorrano, G.; Prato, M. *J. Am. Chem. Soc.* **1997**, *119*, 974.
- Borsenberger, P. M.; Weiss, D. S. *Organic Photoreceptors for Xerography*; Marcel Dekker: New York, 1998.
- Pope, M.; Swenberg, C. E. *Electronic Processes in Organic Crystals*; Oxford University Press: Oxford, U.K., 1999; Chapter 13.
- Salbeck, J. *Anal. Chem.* **1993**, *65*, 2169.
- Brabec, C. J.; Padinger, F.; Dyakonov, V.; Hummelen, J. C.; Janssen, R. A. J.; Sariciftci, N. S. Electronic Properties of Novel Materials—Progress in Molecular Nanostructures. *AIP Conference Proceedings*, 1998; p 519.
- Gao, J.; Hide, F.; Wang, H. *Synth. Met.* **1997**, *84*, 979.